Dynamic Response Estimation and Fatigue Prediction in a Linear Substructure of a Complex Mechanical Assembly

Dimitrios Giagopoulos[1], Alexandros Arailopoulos[1], Saeed Eftekhar Azam[2], Costas Papadimitriou[2], Eleni Chatzi[3], Konstantinos Grompanopoulos[4]

[1] Dept. of Mechanical Engineering, University of Western Macedonia, Kozani, Greece
[2] Dept. of Mechanical Engineering, University of Thessaly, Volos, Greece
[3] ETH Zurich, Inst. of Structural Engineering Dept. Of Civil, Environmental and Geomatic Engineering, Zurich, Switzerland
[4] Public Power Corporation S.A., Meliti Power Plant, Greece

Keywords: FE Model Updating, Strain and Fatigue Predictions, System Identification, Output-Only Measurements.

Abstract

In this work, a computational framework is proposed for online estimation of fatigue damage, in a linear steel substructure of the entire body of a lignite grinder assembly at a PPC power plant. The proposed method is based on sparse vibration measurements and recursive Bayesian filtering for response estimation, in presence of unknown nonstationary excitations. First, a discrete FE model of steel base is developed; the resulting model is then updated for matching its dynamic characteristics with those measured from experiments on a support-free state of the structure. In doing so, measured FRFs are used for estimating the natural frequencies and the damping ratios of the substructure. Structural identification methods are used for estimating the parameters (material properties) of the FE model, based on minimizing the discrepancy between the experimental and analytical modal characteristics, in order to develop a high fidelity FE model. Fatigue is estimated using the Palmgren-Miner damage rule, S-N curves, and rainflow cycle counting of the variable amplitude time histories of the stress components. Incorporating a numerical model of the structure in the response estimation procedure, permits stress estimation at unmeasured spots. Therefore, fatigue estimates could be available at any point on the structure for drawing a complete fatigue map. These stress response characteristics are predicted from by means of a limited number of vibration sensors.

1 INTRODUCTION

The main objective of the present work is to estimate the full strain time histories characteristics at critical locations of a complex mechanical assembly using operational vibration measurements from a limited number of sensors. To achieve this, appropriate numerical and experimental methods were applied, in order to identify, update and optimize the model parameters. In this process, many issues are taken into account, related to the development of FE model, the experimental modal analysis procedure and the development of effective computational model updating techniques.

The output-only vibration measurements during operation in a structure are often recorded by a permanently installed network of sensors. Recently, output-only vibration measurements were proposed to be used for the estimation of fatigue damage accumulation in metallic

components of structures [1]. This is an important safety-related issue in metallic structures since information on fatigue damage accumulation is valuable for designing optimal, cost-effective maintenance strategies and for structural risk assessment. Predictions of fatigue damage accumulation at a point of a structure can be estimated using available damage accumulation models that analyze the actual stress time histories developed during operation [2, 3].

In order to proceed with fatigue predictions, one has to infer the strain/stress response time histories characteristics based on the monitoring information contained in vibration measurements collected from a limited number of sensors attached to a structure. Such predictions are possible if one combines the information in the measurements with information obtained from a high fidelity finite element model of the structure. To optimize the FE model of a structure, structural model updating methods [5], have been proposed in order to reconcile the numerical (FE) model, with experimental data. Structural model parameter estimation based on measured modal data (e.g. [6, 7]) are often formulated as weighted least-squares estimation problems in which metrics, measuring the residuals between measured and model predicted modal characteristics, are build up into a single weighted residuals metric formed as a weighted average of the multiple individual metrics using weighting factors. Standard optimization techniques are then used to find the optimal values of the structural parameters that minimize the single weighted residuals metric representing an overall measure of fit between measured and model predicted modal characteristics. Due to model error and measurement noise, the results of the optimization are affected by the values assumed for the weighting factors.

The organization of this paper is as follows. In section 2, the theoretical formulation of finite element model updating based on modal characteristics and frequency response functions is briefly presented. In the second section, the deterministic and stochastic fatigue damage accumulation formulations are outlined. Next in section 4, presented the experimental application. The modal analysis procedure with the FE model updating examined in the section 4.1, while the effectiveness of the proposed fatigue methodology is demonstrated in the section 4.2. Conclusions are summarized in Section 5.

2 FINITE ELEMENT MODEL UPDATING METHODS

2.1 Modal Residuals

Let $D=\{\hat{\omega}_r, \hat{\underline{\phi}}_r \in R^{N_o}, r=1,\ldots,m\}$ be the measured modal data from a structure, consisting of modal frequencies $\hat{\omega}_r$ and mode shape components $\hat{\underline{\phi}}_r$ at N_o measured DOFs, where m is the number of observed modes. Consider a parameterized class of linear structural models used to model the dynamic behavior of the structure and let $\underline{\theta} \in R^{N\theta}$ be the set of free structural model parameters to be identified using the measured modal data. The objective in a modal-based structural identification methodology is to estimate the values of the parameter set $\underline{\theta}$ so that the modal data $\{\omega_r(\underline{\theta}), \underline{\phi}_r(\underline{\theta}) \in R^{N_0}, r=1,\ldots,m\}$ predicted by the linear class of models at the corresponding N_0 measured DOFs best matches the experimentally obtained modal data in D. For this, let

$$\varepsilon_{\omega_r}(\underline{\theta}) = \frac{\omega_r^2(\underline{\theta}) - \hat{\omega}_r^2}{\hat{\omega}_r^2} \quad \text{and} \quad \varepsilon_{\underline{\phi}}(\underline{\theta}) = \frac{\left\| \beta_r(\underline{\theta}) \underline{\phi}_r(\underline{\theta}) - \hat{\underline{\phi}}_r \right\|}{\left\| \hat{\underline{\phi}}_r \right\|} \tag{1}$$

be the measures of fit or residuals between the measured modal data and the model predicted modal data for the r-th modal frequency and mode shape components, respectively, where $\|\underline{z}\|^2 = \underline{z}^T\underline{z}$ is the usual Euclidean norm, and $\beta_r(\underline{\theta}) = \underline{\hat{\phi}}_r^T \underline{\phi}_r(\underline{\theta}) / \|\underline{\phi}_r(\underline{\theta})\|^2$ is a normalization constant that guaranties that the measured mode shape $\underline{\hat{\phi}}_r$ at the measured DOFs is closest to the model mode shape $\beta_r(\underline{\theta})\underline{\phi}_r(\underline{\theta})$ predicted by the particular value of $\underline{\theta}$. To proceed with the model updating formulation, the measured modal properties are grouped into two groups. The first group contains the modal frequencies while the second group includes the mode shape components for all modes. For each group, a norm is introduced to measure the residuals of the difference between the measured values of the modal properties involved in the group and the corresponding modal values predicted from the model class for a particular value of the parameter set $\underline{\theta}$. For the first group, the measure of fit $J_1(\underline{\theta})$ is selected to represent the difference between the measured and the model predicted frequencies for all modes. For the second group, the measure of fit $J_2(\underline{\theta})$ is selected to represent the difference between the measured and the model predicted mode shape components for all modes. Specifically, the two measures of fit are given by

$$J_1(\underline{\theta}) = \sum_{r=1}^{m} \varepsilon_{\omega_r}^2(\underline{\theta}) \quad \text{and} \quad J_2(\underline{\theta}) = \sum_{r=1}^{m} \varepsilon_{\underline{\phi}_r}^2(\underline{\theta}) = \sum_{r=1}^{m} \left[1 - MAC_r^2(\underline{\theta})\right] \tag{2}$$

where $MAC_r(\underline{\theta}) = \underline{\phi}_r^T \underline{\hat{\phi}}_r(\underline{\theta}) / \|\underline{\phi}_r\| \|\underline{\hat{\phi}}_r\|$ is the Modal Assurance Criterion between experimentally identified and estimated mode shapes for the r-th mode. Alternative measures of fit can easily be used and found in literature [8, 9].

2.2 Modal Residuals

Derived from the MAC for any measured frequency point, ω_k a global correlation coefficient may be used:

$$x_s(\omega_k) = \frac{\left|\{H_X(\omega_k)\}^H \{H_A(\omega_k)\}\right|^2}{\left(\{H_X(\omega_k)\}^H \{H_X(\omega_k)\}\right)\left(\{H_A(\omega_k)\}^H \{H_A(\omega_k)\}\right)} \tag{3}$$

where $\{H_X(\omega_k)\}$ and $\{H_A(\omega_k)\}$ are the experimental (measured) and the analytical (predicted) response vectors at matching excitation - response locations. As the MAC value, $x_s(\omega_k)$ assumes a value between zero and unity and indicates perfect correlation with $x_s(\omega_k) = 1$. For $x_s(\omega_k) = 0$, no correlation exists. Similar to the MAC, $x_s(\omega_k)$ is unable to detect scaling errors and is only sensitive to discrepancies in the overall deflection shape of the structure. To emphasis this characteristic, $x_s(\omega_k)$ is accordingly called the shape correlation coefficient.

The lack of sensitivity to scaling of the shape correlation coefficient does not allow the identification of identical FRFs. This insufficiency becomes even more dramatic if just one measurement and its corresponding prediction are correlated. In this case, the column vectors reduce to scalars and $\{H_A(\omega_k)\} = k\{H_X(\omega_k)\}$ is always satisfied (constant k may be complex), therefore leading to $x_s = 1$ across the full frequency spectrum for uncorrelated FRFs.

As a result, a supplementary correlation coefficient $x_a(\omega_k)$ is proposed by targeting the discrepancies in amplitude. The amplitude correlation coefficient is defined as:

$$x_a(\omega_k) = \frac{2\left|\{H_X(\omega_k)\}^H \{H_A(\omega_k)\}\right|}{\left(\{H_X(\omega_k)\}^H \{H_X(\omega_k)\}\right) + \left(\{H_A(\omega_k)\}^H \{H_A(\omega_k)\}\right)} \tag{4}$$

where the response vectors are identical to those used for $x_s(\omega_k)$. As for the shape correlation coefficient, $x_a(\omega_k)$ is defined to lie between zero and unity. This time, however, the correlation measure is more stringent and only becomes unity if $\{H_A(\omega_k)\} = \{H_X(\omega_k)\}$. That is to say, all elements of the response vectors must be identical in both phase and amplitude even if only one measurement is considered. Similarly, to modal residuals, two measures of fit are proposed using $x_s(\hat{\omega}_r)$ and $x_a(\hat{\omega}_r)$ which correspond to the identified resonant frequencies of the system:

$$J_3(\underline{\theta}) = \sum_{r=1}^{m}\left[1 - x_s(\hat{\omega}_r, \underline{\theta})^2\right] \text{ and } J_4(\underline{\theta}) = \sum_{r=1}^{m}\left[1 - x_a(\hat{\omega}_r, \underline{\theta})^2\right] \tag{5}$$

2.3 Modal Residuals

Minimizing at global minimum the following single objective, traditionally solves the parameter estimation problem:

$$J(\underline{\theta}; \underline{w}) = w_1 J_1(\underline{\theta}) + w_2 J_2(\underline{\theta}) + w_3 J_3(\underline{\theta}) + w_4 J_4(\underline{\theta}) \tag{6}$$

formed by the four objectives $J_i(\underline{\theta})$, using the weighting factors $w_i \geq 0$, $i = 1,2,3,4$, with $w_1 + w_2 + w_3 + w_4 = 1$. The objective function $J(\underline{\theta}; \underline{w})$ represents an overall measure of fit between the measured and the model predicted characteristics. The relative importance of the residual errors in the selection of the optimal model is reflected in the choice of the weights. The results of the identification depend on the weight values used. The optimal solutions for the parameter set $\underline{\theta}$ for given $\underline{w}$ are denoted by $\hat{\underline{\theta}}(\underline{w})$ [10].

3 DETERMINISTIC FATIGUE DAMAGE ACCUMULATION

The Palmgren-Miner rule [2, 3].is commonly used to predict the damage accumulation due to fatigue. According to this rule, a linear damage accumulation law at a point in the structure subjected to variable amplitude stress time history is defined by the formula

$$D = \sum_{i}^{k} \frac{n_i}{N_i} \tag{7}$$

is n_i the number of cycles at a stress level σ_i, N_i is the number of cycles required for failure at a stress level σ_i, and k is the number of stress levels identified in a stress time history at the corresponding structural point. S-N fatigue curves available from laboratory experiments on simple specimens subjected to constant amplitude loads, are used to describe the number of cycles N_i required for failure in terms of the stress level σ_i. The number of cycles n_i at a stress level σ_i is usually obtained by applying stress cycle counting methods, such as the rainflow cycle counting, on the stress time histories measured or estimated for the point under consideration. The fatigue damage accumulation at a point requires that the full stress time histories are available. The fatigue accumulation model can be revised to account for a non-zero mean stress according to the Goodman relationship.

$$\Delta\sigma_{Rt} = \Delta\sigma_R\left(1-\frac{\sigma_m}{\sigma_u}\right) \tag{8}$$

where $\Delta\sigma_{Rt}$ is the modified stress cycle range, $\Delta\sigma_R$ is the original stress cycle range, σ_m is the mean stress, and σ_u is the static strength of the material.

Applying Miner's rule, the fatigue damage of a structural detail depends on the stress range spectrum (stress range $\Delta\sigma$ and number of stress cycles n) and the fatigue detail category classified in the Eurocode 3 as follows:

$$D = \underbrace{\sum_{j=1}^{k_1}\frac{n_i}{5\times10^6}\left(\frac{\Delta\sigma_i}{\Delta\sigma_D}\right)^m}_{\Delta\sigma_i \geq \Delta\sigma_D} + \underbrace{\sum_{j=1}^{k_2}\frac{n_j}{5\times10^6}\left(\frac{\Delta\sigma_j}{\Delta\sigma_D}\right)^{m+2}}_{\Delta\sigma_L \leq \Delta\sigma_j \leq \Delta\sigma_D} \tag{9}$$

where $\Delta\sigma_D$ is the constant amplitude fatigue limit at 5×10^6 cycles; $\Delta\sigma_L$ is the cut-off limit; $\Delta\sigma_i$ and $\Delta\sigma_j$ are the i^{th} and j^{th} stress ranges, n_i and n_j are the number of cycles in each $\Delta\sigma_i$ and $\Delta\sigma_j$ block, and k_1 and k_2 represent the number of different stress range blocks above or below the constant amplitude fatigue limit $\Delta\sigma_D$. In Eurocode 3, each fatigue detail category is designated by a number which represents, in N/mm^2, the reference value $\Delta\sigma_C$ for the fatigue strength at 2 million cycles.

4 EXPERIMENTAL APPLICATION

4.1 Modal Analysis - FE Model Updating

The proposed methodologies are applied in a linear steel frame (secondary base) of the entire body of a lignite grinder assembly at a PPC power plant, which presented in figure 1. In this secondary base, are mounted the support bearing with the rotation shaft of the grinder. This base is mounted, in its turn in the lower main base, in which also mounted the electric motor. First, the geometry of the steel frame of the secondary base is discretized mainly by solid (tetrahedral) elements. The total number of DOFs was about 2,500,000. The detailed FE model is presented in Figure 2. For the development and solution of the finite element model using appropriate software [13, 14].

After developing the nominal finite element model, an experimental modal analysis of the steel frame, was performed in order to quantify its dynamic characteristics. The base was hung up using a crane and straps, to approximate free-free boundary conditions for the test. First, all the necessary elements of the FRF matrix required for determining the response of the substructures were determined by imposing impulsive loading. The measured frequency range was 0-2048 Hz, which includes the analytical frequency range of interest for the base frame, 0-100 Hz. An initial investigation indicated twelve natural frequencies for the frame, in this frequency range. A schematic illustration of the experimental arrangement is presented in Figure 3. In this figure, the locations and directions of acceleration measurements are presented, applying an impulsive load in all directions and at several locations. Based on the measured FR functions, the natural frequencies and the damping ratios of the substructures were estimated [10, 12]. The identified mode shapes have also been recorded so that they can be used for updating the finite element model.

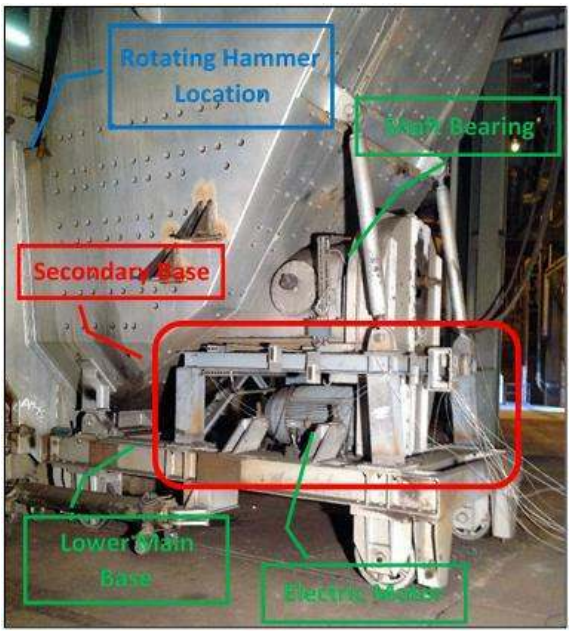

Figure 1: Entire body of a lignite grinder assembly.

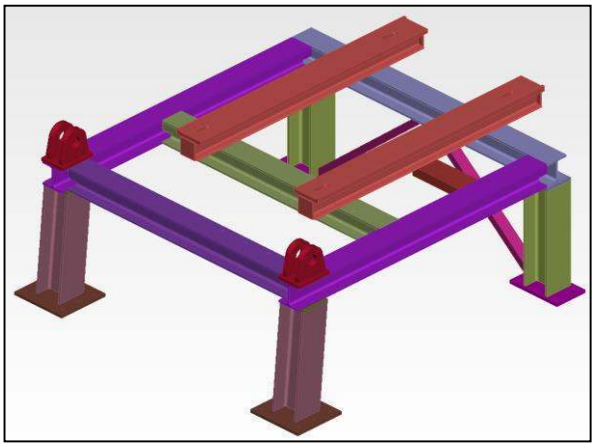

Figure 2: Finite element model of the secondary base.

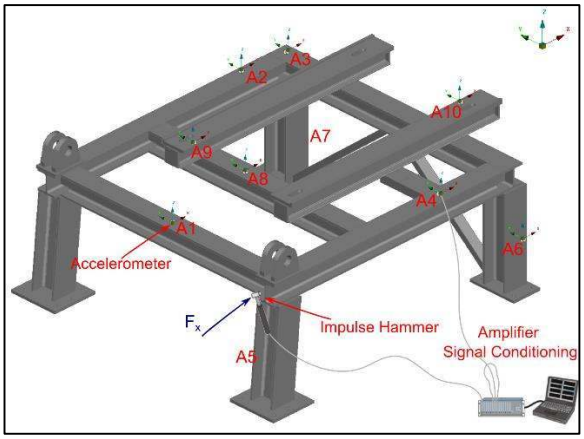

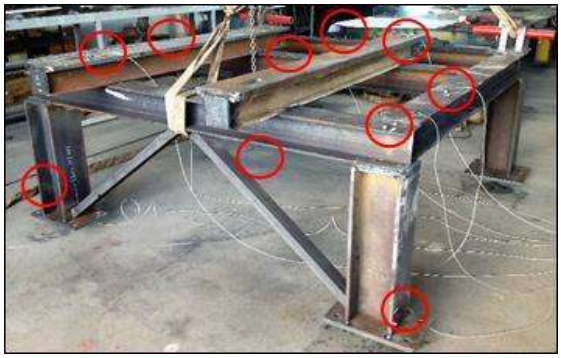

Figure 3: Accelerometer locations on base frame.

As an outcome of the above procedure, in the Table 1 summarized the modal analysis results for the base frame. More specifically, the first column of Table 1 presents the values of the lowest natural frequencies (ω_{rE}), while the corresponding damping ratios are included in the fourth column. In the same table, the second column presents the values of the natural frequencies obtained from the analysis of the nominal finite element model $(\omega_{r\,N_{FE}})$ and the third column compares these frequencies with the corresponding frequencies obtained by the experimental data. The errors determined between the nominal FE model and the experimental measurements are not insignificant, indicating that the FE model updating process is necessary.

The parameterization of the finite element model is introduced in order to demonstrate the applicability of the proposed finite element model updating method. The parameterized models are consisted of fourteen parts, as shown in Figure 4. All parts are modeled with solid elements. The Young's modulus and the density are used as design variables. Thus, the final numbers of

the design parameters are twenty-eight (28). The FE model of the frame is updated using the identified FRFs, modal frequencies and mode shapes shown in Tables 1.

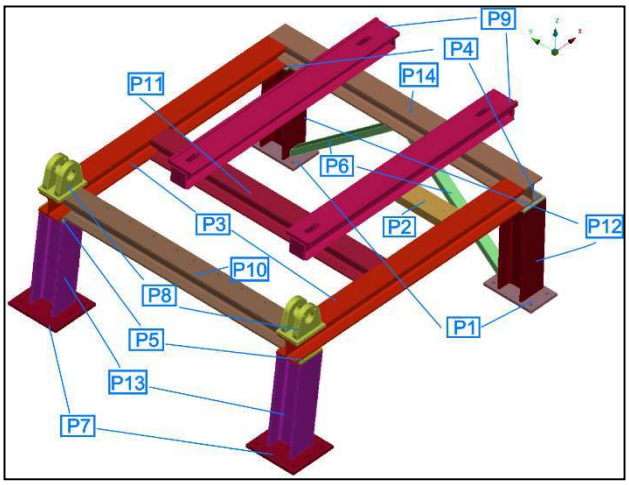

Figure 4: Entire body of a lignite grinder assembly.

Mode	Identified Modal Frequency	Nominal FE Predicted Modal Frequency	Difference between Identified and FE Predicted Modal Frequencies	Identified Modal Damping Ratio
	ω_{rE} [Hz]	$\omega_{rN_{FE}}$ [Hz]	$\frac{\omega_{rN_{FE}} - \omega_{rE}}{\omega_{rN_{FE}}} 100\%$	ζ_{rE} (%)
1	7.10	8.53	16.81	0.08
2	41.71	44.01	5.23	0.02
3	42.70	47.09	9.31	0.56
4	43.82	47.63	8.00	0.02
5	45.46	49.72	8.58	0.37
6	59.71	64.03	6.75	0.09
7	64.23	70.19	8.49	0.05
8	72.36	77.96	7.18	0.22
9	73.72	81.86	9.94	0.04
10	75.02	84.51	11.24	0.31
11	77.37	90.13	14.15	0.08
12	78.09	90.59	13.79	0.12

Table 1: Modal frequencies and modal damping ratios of the frame.

In Table 2 presented the initial values that have been set in each parameter, which are identical to the nominal FE model, with the upper and lower limits, which were selected to be used for the optimization process.

Part	Initial Density [kg/m^3]	Initial Young's Modulus [Gpa]	Move Limit	Part	Initial Density [kg/m^3]	Initial Young's Modulus [Gpa]	Move Limit
	LB - UB	LB - UB			LB - UB	LB - UB	
P1	7850 **6050-9660**	210 **160-230**	1%	P8	6050-9660 **7850**	160-230 **210**	1%
P2	168 **7850**	**210**	1%	P9	6050-9660 **7850**	160-230 **210**	1%
P3	6050-9660 **7850**	160-230 **210**	1%	P10	6050-9660 **7850**	160-230 **210**	1%
P4	6050-9660 **7850**	160-230 **210**	1%	P11	6050-9660 **7850**	160-230 **210**	1%
P5	6050-9660 **7850**	160-230 **210**	1%	P12	6050-9660 **7850**	160-230 **210**	1%
P6	6050-9660 **7850**	160-230 **210**	1%	P13	6050-9660 **7850**	160-230 **210**	1%
P7	6050-9660 **7850**	160-230 **210**	1%	P14	6050-9660 **7850**	160-230 **210**	1%

Table 2: Design variables and optimization design limits.

The results from the FE model updating method are shown first in Table 3. In this table presented a comparison between identified (ω_{rE}) and optimal FE predicted modal frequencies $(\omega_{rO_{FE}})$. The FRF predicted by the optimal FE model (black dashed line) for the frame are compared in Figure 5 with the FRF computed directly from the measured data (red continuous line) at one indicative measurement location in the frequency range [0Hz, 90Hz]. The FRF of the initial nominal model (blue dashed dot line) is also shown in this figure. Compared to the FRF of the initial nominal model, it is observed that the updated optimal model tends to considerably improve the fit between the model predicted and the experimentally obtained FRF close to the resonance peaks.

Mode	Identified Modal Frequency	Optimal FE Predicted Modal Frequency	Difference between Identified and FE Predicted Modal Frequencies
	ω_{rE} [Hz]	$\omega_{rO_{FE}}$ [Hz]	$\frac{\omega_{rO_{FE}} - \omega_{rE}}{\omega_{rO_{FE}}} 100\%$
1	7.10	7.29	2.60
2	41.71	41.36	0.86
3	42.70	42.12	1.39
4	43.82	42.55	2.98
5	45.46	44.80	1.46
6	59.71	59.57	0.23
7	64.23	63.96	0.42
8	72.36	71.45	1.28
9	73.72	72.72	1.37
10	75.02	75.22	0.26
11	77.37	78.30	1.19
12	78.09	78.69	0.75

Table 3: Comparison between identified and optimal FE predicted modal frequencies

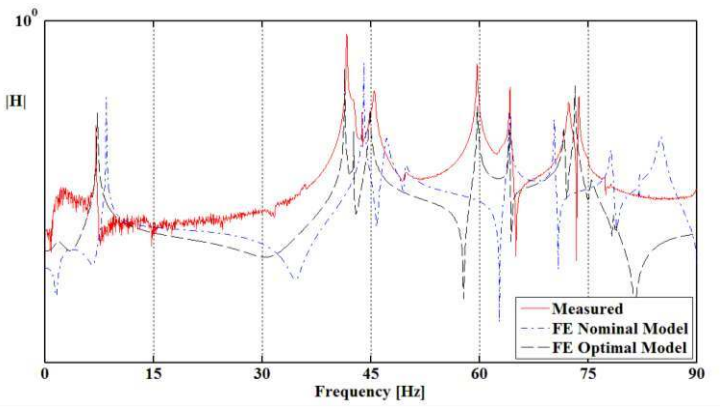

Figure 5: Comparison between measured, nominal and optimal FRF in a typical element of the FRF matrix..

4.2 Fatigue Monitoring using operational vibrations

After testing the reliability of the base frame FE model, the stresses under real dynamic load conditions were calculated. The ultimate aim was the identification of those points where the larger stresses appear. To achieve this, using acceleration (triaxial) measurements at a limited number of locations (10). A schematic illustration of the experimental arrangement is presented in Figure 6.

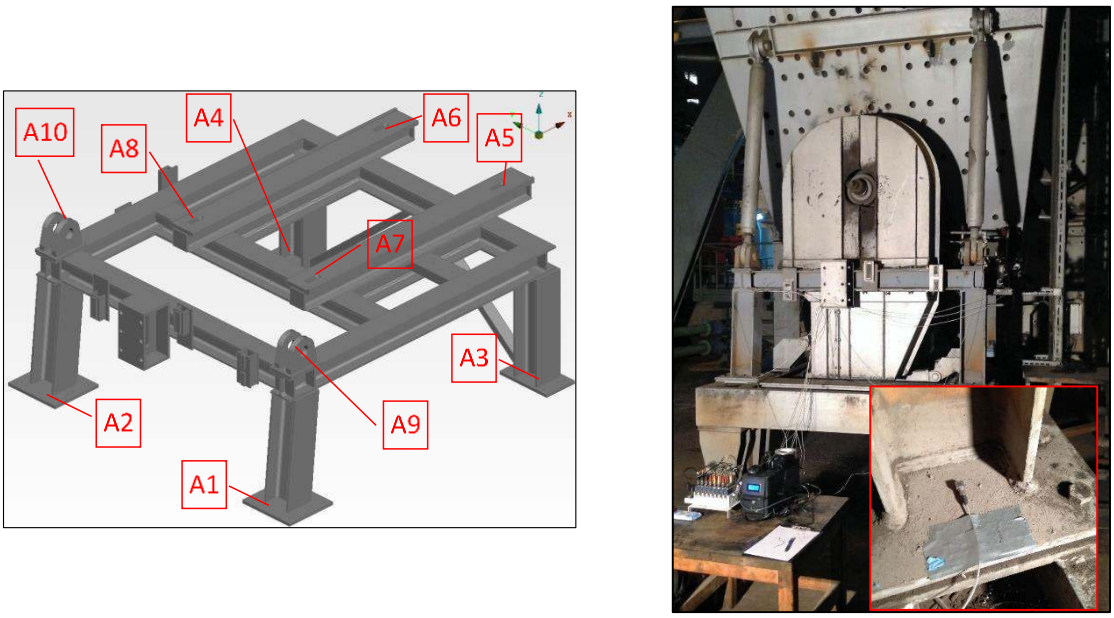

Figure 6: Accelerometer locations on base frame in real operating conditions.

Incorporating the measured acceleration time histories in the numerical model of the frame, the model was solved in order to calculate the maximum stresses developed. Figure 7 shows

selected results, in which some indicative points (ST1-ST4) of the superstructure with maximum stresses are presented.

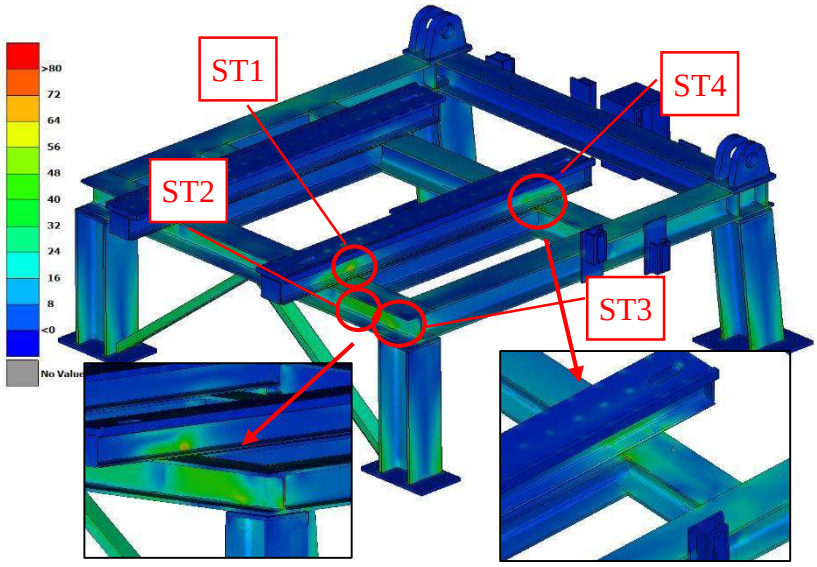

Figure 7: Locations of the frame where maximum stresses appear.

Finally, using the calculated stress time histories at locations (ST1-ST4) and utilizing the available S-N fatigue curves, the Miner's rule is applied to estimate the fatigue damage accumulation. The frame is made of steel and the fatigue detail category 36 is adopted to illustrate the method. The static strength of steel is assigned the value $\sigma_u = 440$ MPa. According to Eurocode 3 for detail category 36, the following values of the parameters of the design S-N curves are recommended: $m = 3$, $\Delta\sigma_D = 26.5$ MPa and $\Delta\sigma_L = 14.5$ MPa.

The calculated fatigue life for the four locations are presented in Table 4. The results of numerical analysis were confirmed from the real structure. More specifically, the photo in Figure 8, presents the crack in the frame, exactly in the same locations (ST2-ST3) where the numerical analysis results show. Also, this crack appeared only in 60 days from the time that the base put into operation. This value is very close to the results presented in Table 4. These results indicate that the methodology applied gives accurate results and provides a useful tool in predicting the fatigue damage accumulation.

Location	Calculated Fatigue Life (Days)
ST1	35.64
ST2	65.85
ST3	58.96
ST4	269.35

Table 4: Calculated Fatigue Life

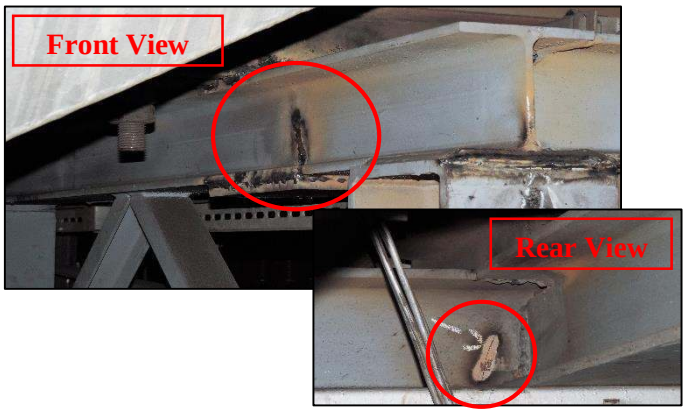

Figure 8: Crack in the real frame.

5 CONCLUSIONS

A computational framework is proposed for estimating fatigue damage accumulation in a linear steel substructure of the entire body of a lignite grinder assembly at a PPC power plant. This is accomplished by combining fatigue damage accumulation laws with stress/strain predictions based on output only vibration measurements collected from a limited number of sensors. Methods for estimating strains by integrating high fidelity finite element model and estimation techniques were summarized. From the results is clear that fatigue damage is estimated, a fact that reveals that the methodology for estimating damage due to fatigue on the entire body of a structure by combining linear damage accumulation laws, S-N fatigue curves, rainflow cycle-counting algorithms, and acceleration measurements at a limited number of locations is a valuable tool for designing optimal fatigue-based maintenance strategies in a wide variety of structures.

REFERENCES

[1] C. Papadimitriou, C. P. Fritzen, P. Kraemer, and E. Ntotsios, "Fatigue predictions in entire body of metallic structures from a limited number of vibration sensors using Kalman filtering," Structural Control and Health Monitoring, vol. 18, pp. 554-573, 2011.

[2] A. Palmgren, "Die Lebensdauer von Kugallagern," VDI-Zeitschrift, vol. 68, pp. 339-341, 1924.

[3] M. A. Miner, "Cumulative damage in fatigue," Applied Mechanics Transactions (ASME), vol. 12, pp. 159-164, 1945.

[4] Mottershead, J.E. and Friswell, M.I., Model updating in structural dynamics: A survey, Journal of Sound and Vibration, Vol. 167, pp. 347-375, 1997.

[5] Giagopoulos, D. and Natsiavas, S., Dynamic Response and Identification of Critical Points in the Superstructure of a Vehicle using a Combination of Numerical and Experimental Methods, Experimental Mechanics, Vol. 55, pp. 529-542, 2015.

[6] Spottswood, S.M. and Allemang, R.J., On the investigation of some parameter identification and experimental modal filtering issues for nonlinear reduced order models, Experimental Mechanics, Vol. 47, pp. 511-521, 2007.

[7] Fritzen CP, Jennewein D, Kiefer T. Damage detection based on model updating methods. Mechanical Systems and Signal Processing 1998; 12(1):163–186.

[8] Yuen K-V, Beck JL, Katafygiotis LS. Efficient model updating and health monitoring methodology using incomplete modal data without mode matching. Structural Control and Health Monitoring 2006; 13:91–107.

[9] Papadimitriou, C., Ntotsios, E., Giagopoulos, D. and Natsiavas, S., Variability of updated finite element models and their predictions consistent with vibration measurements, Structural Control and Health Monitoring, Vol. 19, pp. 630-654, 2012.

[10] Arailopoulos, A., Giagopoulos, D., Finite Element Model Updating Techniques of Complex Assemblies with Linear and Nonlinear Components, Proceedings of the IMAC-XXXIV 2016, Orlando, Florida, USA, 2016.

[11] Ntotsios E, Papadimitriou C. Multi-objective optimization algorithms for finite element model updating. International Conference on Noise and Vibration Engineering (ISMA2008); Katholieke Universiteit Leuven, Leuven, Belgium, September 15-17, 2008.

[12] Ewins, D.J., 1984, Modal Testing: Theory and Practice, Research Studies Press, Somerset, England.

[13] DYNAMIS 3.1.1, Solver Reference Guide, DTECH, Thessaloniki, Greece, 2016.

[14] ANSA and META-Post, BETA CAE Systems S.A., Thessaloniki, Greece.